IJST (2015) 39A3: 243-251
Iranian Journal of Science & Technology

http://ijsts.shirazu.ac.ir

Image denoising based on approximate solution of fractional Cauchy-Euler equation by using complex-step method

R. W. Ibrahim* and H. A. Jalab

Faculty of Computer Science and Information Technology, University Malaya, 50603, Malaysia
E-mails: rabhaibrahim@yahoo.com & hamidjalab@um.edu.my

Abstract

The complex-step derivative approximation is applied to compute numerical derivatives. In this study, we propose a new formula of fractional complex-step method utilizing Jumarie definition. Based on this method, we illustrated an approximate analytic solution for the fractional Cauchy-Euler equations. Application in image denoising is imposed by introducing a new fractional mask depending on such a solution.

Keywords: Fractional calculus; fractional differential equations; fractional differential operator; analytic function

1. Introduction

Recently, the complex-step method has been considered by many researchers (Abreu, Stich, & Morales, 2013) (Al-Mohy & Higham, 2010). The advantages of the complex-step approximation method over a typical finite difference include: 1) it can be employed on discontinuous functions, 2) the Jacobian approximation is not related to subtractive cancelations inherent on roundoff errors, 3) it can be utilized near analytical accuracy caused by an arbitrarily small step-size and 4) it can be assumed in general non-linear functions. Ibrahim introduced the fractional complex transform, convert fractional differential equations analytically in the sense of the Srivastava-Owa fractional operator and its generalization in the unit disk (Ibrahim, 2011, 2012). Jumarie studied fractional Brownian motion with complex variables (Jumarie, 2006). The authors generalized the complex-step method by utilizing the fractional calculus differential operator. They derived several approximations for computing the fractional order derivatives. Stability of the generalized fractional complex step approximations is deduced for analytic test functions (Ibrahim & Jalab, 2013).

The most recent applications of fractional calculus occur in signal and image processing. The differential operators were used in the sense of Riemann-Liouville operator, Srivastava-Owa operator and its generalization, Grünwald-Letnikov operator and ells. Moreover, the authors employed the fractional polynomials such as Alexander and Conway polynomials (Jalab & Ibrahim, 2012, 2015a, 2015b). In this study we shall focuss on discrete fractional operators in the sense of Jumarie derivative The complex-step derivative approximation is applied to compute numerical derivatives. In this work, we propose a new rule of fractional complex-step method by making use of Jumarie definition. Based on this method, an approximate analytic solution for the fractional Cauchy- Euler equations was clarified. Application in image denoising is imposed by introducing a new fractional mask depending on such a solution.

2. Main method

This section deals with preliminaries and some concepts(Jumarie, 2006).

Definition 2.1. For a continuous function $\phi:\mathsf{R}\to\mathsf{R}$ and a constant $\hbar>0,$ the forward operator $FW(\hbar)$ is defined by the equality

$$FW(\hbar)\phi(x):=\phi(x+\hbar).$$

The fractional difference on the right and of order $\wp,0<\wp<1$ of $\phi(x)$ is defined by the formula

$$\Delta_J^{\wp}\phi(x):=(FW(\hbar)-1)^{\wp}\phi(x)$$

with its fractional derivative on the right

$$\phi_+^{(\wp)}(x)=\lim_{\hbar\to 0}\frac{\Delta_J^{\wp}[\phi(x)-\phi(0)]}{\hbar^{\wp}}.$$

*Corresponding author
Received: 16 September 2014 / Accepted: 11 March 2015

The fractional Taylor expansion is obtained by the following formula:

$$\phi(x+\Delta x)=\phi(x)+D_x^{\wp}\phi(x)\frac{(\Delta x)^{\wp}}{\Gamma(\wp+1)}+D_x^{\wp}D_x^{\wp}\phi(x)\frac{(\Delta x)^{2\wp}}{\Gamma(2\wp+1)}+\cdots+D_x^{n\wp}\phi(x)\frac{(\Delta x)^{n\wp}}{\Gamma(n\wp+1)}, \quad (1)$$

where $D_x^{\wp}$ is the Riemann-Liouville differential operator, $\Delta x_{k-1}:=x_k-x_{k-1}$ is the forward deference operator and

$$D_x^{n\wp}:=\underbrace{D_x^{\wp}D_x^{\wp}..D_x^{\wp}}_{n-times}.$$

Applying Definition 2.1 on (1), yields

$$\phi(x+\Delta x)=\phi(x)+\phi^{(\wp)}(x)\frac{(\Delta_J x)^{\wp}}{\Gamma(\wp+1)}+\phi^{(2\wp)}(x)\frac{(\Delta_J x)^{2\wp}}{\Gamma(2\wp+1)}+\cdots+\phi^{(n\wp)}(x)\frac{(\Delta_J x)^{n\wp}}{\Gamma(n\wp+1)}, \quad (2)$$

where

$$(\Delta_J)^{n\wp}:=\underbrace{\Delta_J^{\wp}\Delta_J^{\wp}..\Delta_J^{\wp}}_{n-times}.$$

The authors constructed the fractional complex step method (FCSM), employing the function $\phi(x+\sqrt[\wp]{i}\Delta x),\wp\in(0,1),$ and deduced the approximation of the fractional derivative

$$D_x^{\wp}\phi(x)=\frac{\Gamma(\wp+1)\Im[\phi(x+\sqrt[\wp]{i}\Delta x)]}{(\Delta x)^{\wp}}+\Theta(\Delta x^{\wp}), \quad (3)$$

where $\Theta(\Delta x^{2\wp})$ is the error. While the approximation of the second fractional derivative $D^{2\wp}$ is defined as follows:

$$D_x^{2\wp}\phi(x)=-\frac{\Gamma(2\wp+1)\Re[\phi(x+\sqrt[\wp]{i}\Delta x)-\phi(x)]}{(\Delta x)^{2\wp}}+\Theta(\Delta x^{2\wp}). \quad (4)$$

Moreover, the authors generalized the above approximations by employing the function $\phi(x+u+\sqrt[\wp]{i}v),$ where u and v are real numbers related to the real and imaginary differential steps, by

$$D_x^{\wp}\phi(x)=\frac{\Gamma(\wp+1)\Im[\phi(x+u+\sqrt[\wp]{i}v)]}{v^{\wp}}+\Theta(u^{\wp},v) \quad (5)$$

and

$$D_x^{2\wp}\phi(x)=\frac{\Gamma(2\wp+1)\Im[\phi(x+u+\sqrt[\wp]{i}v)]}{v^{2\wp}}+\Theta(u^{2\wp},v).$$

Other versions can be found in (Ibrahim & Jalab, 2013).

Applying the Jumarie deference, on (3) and (4) to obtain the modify fractional complex-step method

$$\phi^{(\wp)}(x)=\frac{\Gamma(\wp+1)\Im[\phi(x+\sqrt[\wp]{i}\Delta_J x)]}{(\Delta_J x)^{\wp}}+\Theta(\Delta_J x^{\wp}),\quad 0<\wp<1, \quad (6)$$

where $\Theta(\Delta_J x^{\wp})$ is the error. While the approximation of the second fractional derivative is defined as follows:

$$\phi^{(2\wp)}(x)=-\frac{\Gamma(2\wp+1)\Re[\phi(x+\sqrt[\wp]{i}\Delta_J x)-\phi(x)]}{(\Delta_J x)^{2\wp}}+\Theta(\Delta_J x^{2\wp}),\quad 0<\wp<1. \quad (7)$$

3. Main outcomes

In this section, we deal with an approximate solution for the fractional Cauchy-Euler equation

$$z^2\phi^{(2\wp)}(z)+2(1+\mu)z\phi^{(\wp)}(z)+\mu(1+\mu)=(1+\mu)(2+\mu)\psi(z),\quad 0<\wp<1 \quad (8)$$

where $\mu\in\mathbb{R}\setminus(-\infty,-1]$, ϕ and ψ are analytic functions belonging to the class $\mathbb{A}$ of functions

$$\sigma(z)=z+\sum_{n=2}^{\infty}\varsigma_n z^n,\quad z\in U:=\{z:|z|<1\}. \quad (9)$$

The class $\mathbb{A}$ is the main class of functions in the theory of univalent function. It is well known that if $|\varsigma_n|\le n,$ then the function is univalent and if $|\varsigma_n|\le 1,$ then the function is convex.

Next we investigate the univalent and convex univalent solutions of the problem (8), for $\wp\to 1.$

Theorem 3.1. Assume that $\phi,\psi\in\mathbb{A}$ are in the class $S^*(b),b\in\mathbb{C}^*=\mathbb{C}\setminus\{0\}$ satisfying

$$\Re\{1+\frac{1}{b}(\frac{z\phi'(z)}{\phi(z)}-1)\}>0.$$

If $\mu=0$ and b satisfies the inequality

$$|b|\le\frac{n!-\prod_{j=0}^{n-2}j}{2}$$

then Eq. (8) has a univalent solution in the unit disk.

Proof: Let the functions ϕ and ψ be in the class $S^*(b)$. Thus they achieve the relation [19]

$$|\varsigma_n|\le\frac{\prod_{j=0}^{n-2}j+2|b|}{(n-1)!}.$$

By the assumption, we conclude that

$$|\varsigma_n|\le n,$$

consequently, (8) has a univalent solution.

Theorem 3.2. Assume that $\phi\in A$ and $\psi\in A$ is in the class $\mathcal{B}^*(m,\lambda,\wp,b),b\in\mathbb{C}^*=\mathbb{C}\setminus\{0\}$ satisfying

$$\Re\{1+\frac{1}{b}(\frac{z[(1-\lambda)D^m\psi(z)+\lambda D^{m+1}\psi(z)]'}{(1-\lambda)D^m\psi(z)+\lambda D^{m+1}\psi(z)}-1)\}>\wp,$$

where D^m is the Salagean operator (Salagean, 1983). If b satisfies the inequality

$$|b|\le\frac{n!n^m(1-\lambda+n\lambda)(n+\mu)(n+1+\mu)-\prod_{j=0}^{n-2}j(1+\mu)(2+\mu)}{2(1-\wp)(1+\mu)(2+\mu)}$$

$$(\mu\in\mathbb{R}\setminus\{-1,-2\},0<\wp<1,0\le\lambda\le1)$$

then Eq. (8) has a univalent solution in the unit disk.

Proof: Let

$$\phi(z)=z+\sum_{n=2}^{\infty}\varsigma_n z^n,\quad \psi(z)=z+\sum_{n=2}^{\infty}\alpha_n z^n.$$

Since $\psi\in\mathcal{B}^*(m,\lambda,\wp,b),$ then we obtain

$$|\alpha_n|\le\frac{\prod_{j=0}^{n-2}j+2|b|(1-\wp)}{(n-1)!n^m(1-\lambda+n\lambda)}.$$

Moreover, we have

$$\varsigma_n=\frac{(1+\mu)(2+\mu)}{(n+\mu)(n+1+\mu)}\alpha_n,$$

thus we attain

$$|\varsigma_n|\le\frac{(1+\mu)(2+\mu)[\prod_{j=0}^{n-2}j+2|b|(1-\wp)]}{(n-1)!n^m(1-\lambda+n\lambda)(n+\mu)(n+1+\mu)}.$$

By the hypotheses of the theorem we get

$|\varsigma_n|\le n,$

which implies that (8) admits a univalent solution.

We proceed to study the convex univalent solutions of the problem (8).

Theorem 3.3. Assume that $\phi,\psi\in A$ are in the class $C(b),b\in\mathbb{C}^*=\mathbb{C}\setminus\{0\}$ satisfying

$$\Re\{1+\frac{1}{b}(\frac{z\phi''(z)}{\phi'(z)}-1)\}>0.$$

If $\mu=0$ and b achieves the inequality

$$|b|\le\frac{n!-\prod_{j=0}^{n-2}j}{2}$$

then Eq. (8) has a univalent solution in the unit disk.

Proof: Let the functions ϕ and ψ be in the class $S^*(b)$. Thus, we have

$$|\varsigma_n|\le\frac{\prod_{j=0}^{n-2}j+2|b|}{n!}.$$

By the assumption, we conclude that

$$|\varsigma_n|\le1,$$

consequently, (8) has a convex univalent solution.

4. Applications

Recently, fractional calculus was applied in image processing procedures. This technique is divided into two branches: fractional differentiation and fraction integration operators. In our discussion, we utilize the approximate solution of (8). By applying the approximate fractional derivatives (6) and (7) in

(8), we may conclude that for $\mu = 0,\ \hbar \to 1,$ and the function $\psi(z) = \wp\Gamma(\wp+1)z,$ the approximate solution of (8) takes its form $\phi(z) \approx z$.

The fractional Cauchy-Euler equation (FCE) mask windows can be applied on four directions. We conduct a convoluting FCE filter on four directions. These directions are used to cover all corrupted pixels inside the corrupted image. To address this situation, we define the fractional mask windows on four directions (θ), namely 0°, 45°, 90°, and 135° (Fig. 1).

$Mask_1$ $Mask_2$

0	θ_2	0
0	θ_1	0
0	θ_0	0

0	0	0
θ_0	θ_1	θ_2
0	0	0

$Mask_3$ $Mask_4$

0	0	θ_2
0	θ_1	0
θ_0	0	0

θ_0	0	0
0	θ_1	0
0	0	θ_2

Fig. 1. Fractional Differential masks on 4 directions: 90°, 0°, 45°, and 135°

To achieve high denoising with low complexity, the size of the mask window should be small. The steps for the proposed image denoising algorithm of the fractional mask window is presented as follows:

1. FCE windows with 3 × 3 sizes are initialized.
2. The values of the fractional power of the proposed mask windows with ranges of $\wp \in (0,1).$
3. Additive white Gaussian noise with standard deviation of 15, 20, 25 and 30 are added to test the performance of the proposed algorithm.
4. Each pixel of the $f(i,j)$ corrupted images are convolved with the mask windows using the following technique:

$$Denoised\,image = \frac{1}{4}\sum_{k=1}^{4} mask_k * f(i,j) \quad (10)$$

5. Gaussian filter, and proposed filter were then applied to the corrupted images to remove the noise.
6. The performance of the denoising process was quantified using the peak signal to noise ratio (PSNR)(Jalab & Ibrahim, 2012).

The same algorithm can be utilized for color images, but is implemented separately for each of the red, green, and blue color components.

4. 1. Experimental results

This section demonstrates the denoising performance of FCE. Performance tests are implemented by using MATLAB 2013b on Windows 8.1. The following sets of grayscale images of size 256 × 256 pixels are employed in this: "Lena", "" X- Ray", "Boat" and "MRI image". We study the performance of the proposed approach by using images corrupted by additive white Gaussian noise with standard deviation σ values of 15, 20, 25 and 30. To verify the quality of the denoised image we consider PSNR, which has been widely used in literature to determine the quality of a processed image (Jalab & Ibrahim, 2012). The optimal value of fractional power parameter $\wp < 1$, was defined depending on the relation between PSNR and $\wp$ using "Lena" corrupted by additive white Gaussian noise with a standard deviation σ of 15. From Fig 2, we can reach the following conclusions: The PSNR reaches peak value in 0.8 for FCE algorithm. While, the PSNR decreases rapidly as $\wp$ tends to 1.

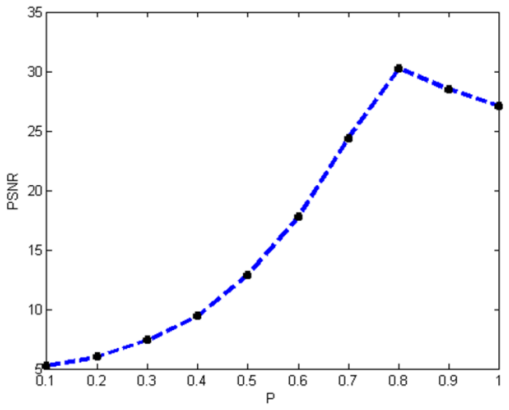

Fig. 2. PSNR with different choices of parameter *P* for "Lena" corrupted by additive white Gaussian noise of standard deviation σ = 15

The experimental results of all images are shown in Figs. 3 to 6. These figures show the proposed FCE algorithm has good denoising performance for all testing images. Figures 7-10 show the results of the PSNR obtained with different values of α for "Lena", " X- Ray", "Boat" and MRI respectively. The maximum PSNR value is obtained by our proposed algorithms by using the optimal values of α. The denoised PSNR results of our proposed algorithms are higher than that of the Gaussian for higher noise level.

Fig. 3. Experiment for "Lena". (a) original image. (b) corrupted image by Gaussian noise for σ=10, 20 and 30. (c) Gaussian smoothing filter. (d) FCE proposed filter

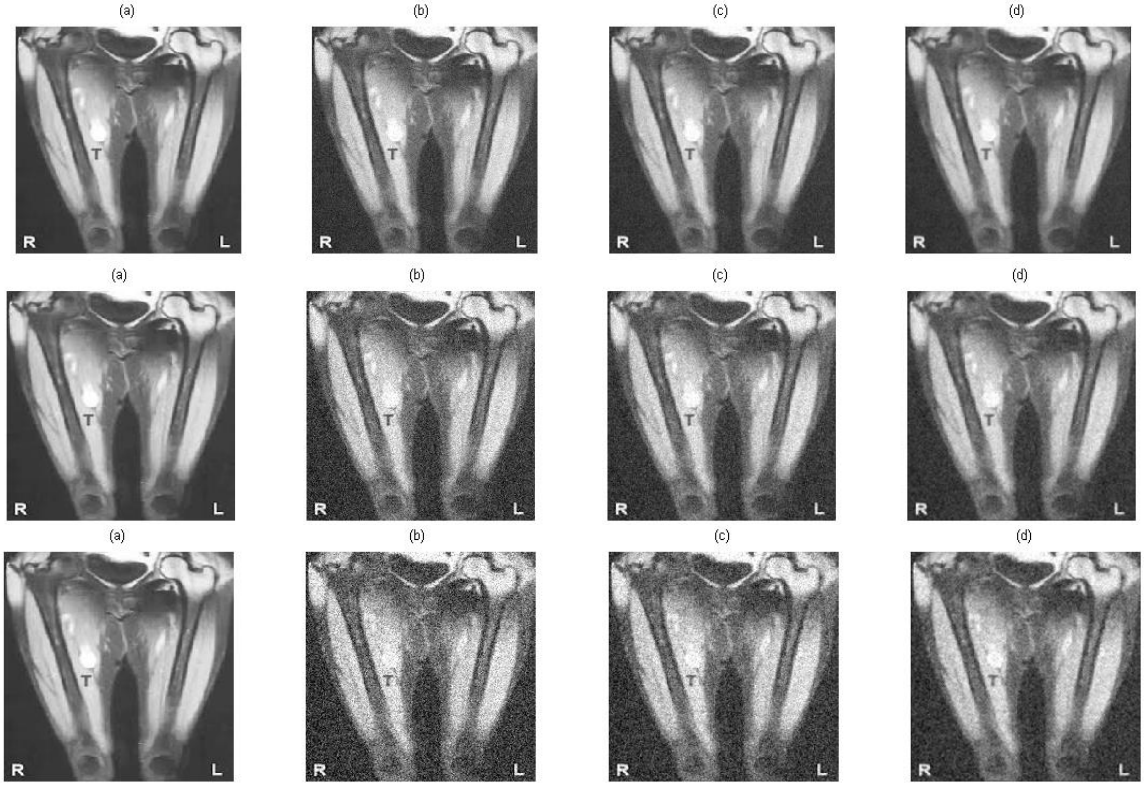

Fig. 4. Experiment for "X- Ray". (a) original image. (b) corrupted image by Gaussian noise for σ=10, 20 and 30. (c) Gaussian smoothing filter. (d) FCE proposed filter

Fig. 5. Experiment for "Boat". (a) original image. (b) corrupted image by Gaussian noise for σ=10, 20 and 30. (c) Gaussian smoothing filter. (d) FCE proposed filter

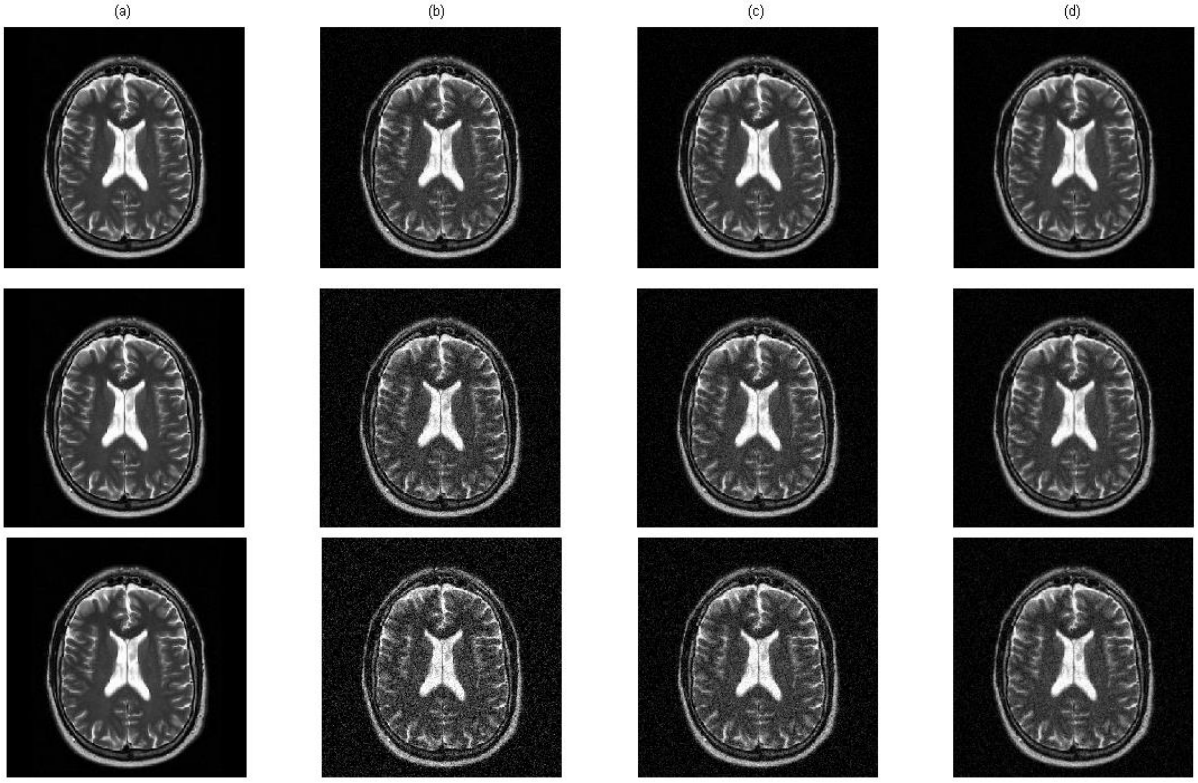

Fig. 6. Experiment for "MRI" (a) original image. (b) corrupted image by Gaussian noise for σ=10, 20 and 30. (c) Gaussian smoothing filter. (d) FCE proposed filter

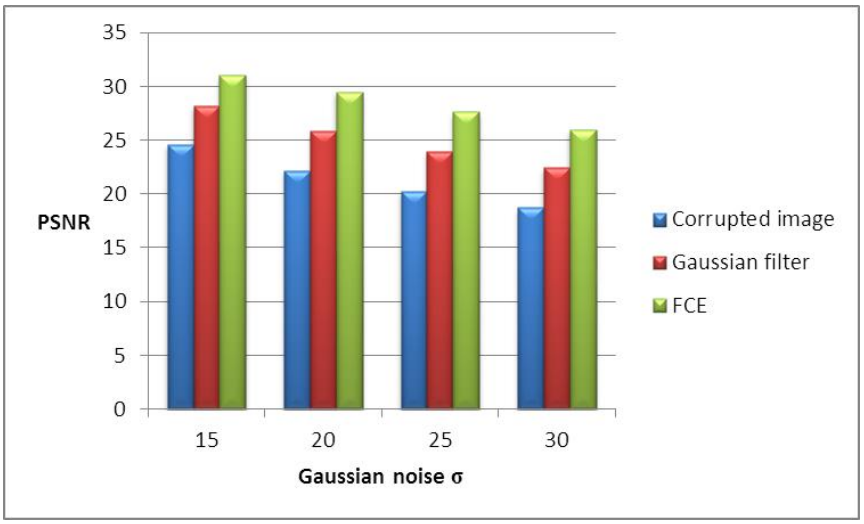

Fig. 7. Experimental results of the PSNR for "Lena" obtained with Gaussian noise σ=10, 20 and 30

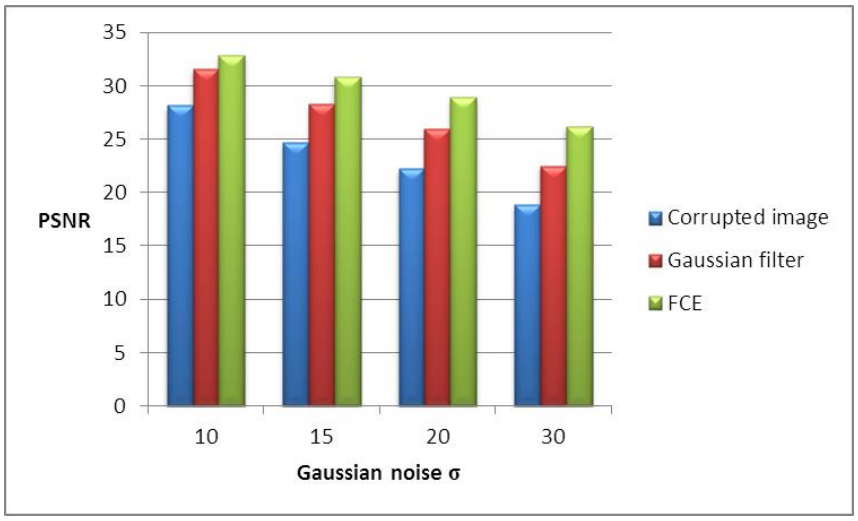

Fig. 8. Experimental results of the PSNR for "X-Ray" obtained with Gaussian noise σ=10, 20 and 30

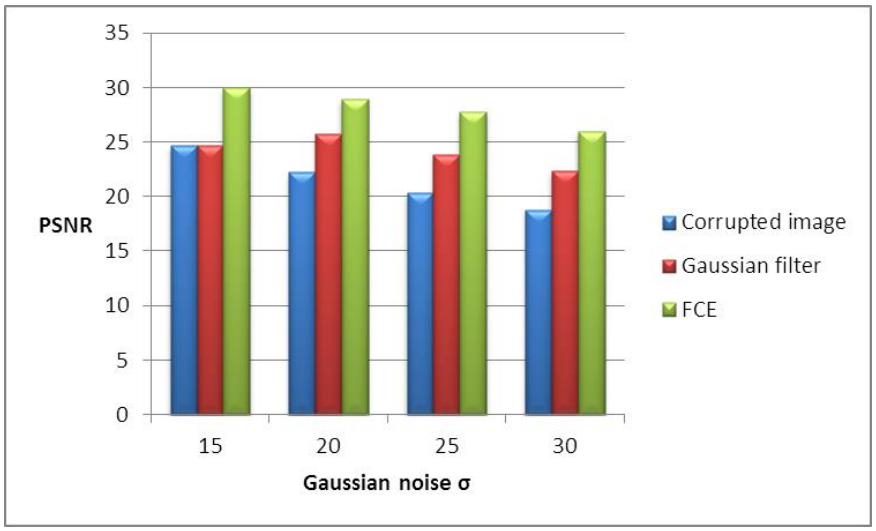

Fig. 9. Experimental results of the PSNR for "Boat" obtained with Gaussian noise σ=10, 20 and 30

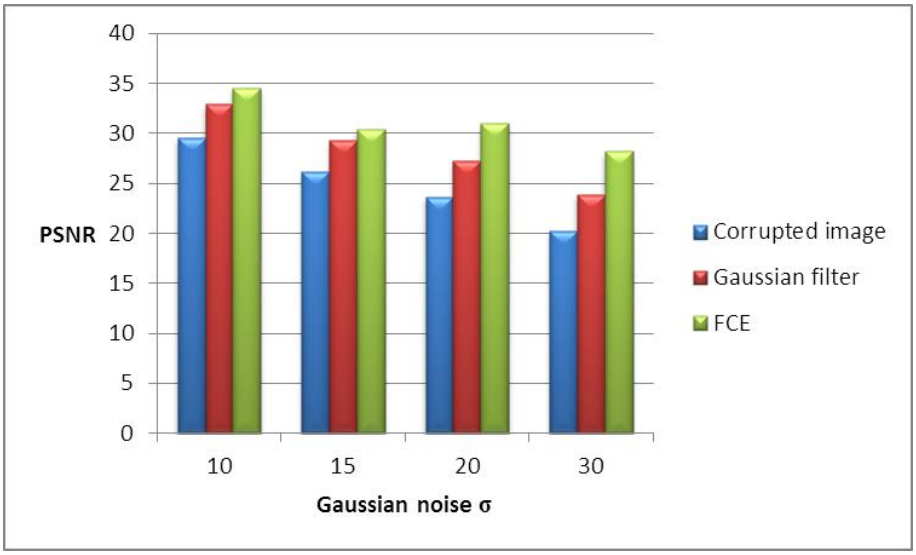

Fig. 10. Experimental results of the PSNR for "MRI" obtained with Gaussian noise σ=10, 20 and 30

4. 2. Comparison with other methods

Table 1 shows the comparison of the experimental results for "Boat" of the proposed algorithm with other denoising algorithms based on fractional calculus. Jalab and Ibrahim (2012) proposed an image denoising algorithm called generalized fractional integral filter based on generalized Srivastava-Owa fractional integral operator. Cuesta, Kirane, & Malik (2012) proposed a partial differential equation based on Volterra equation as a pixel-by-pixel technique for filtering, denoising, and enhancing. Table 1 provides an overall view of the performance of different methods, although these methods use the same image with different noise σ values. The values of PSNR for FCE is slightly higher than those for the other methods for noise σ values of 15, 20, and 25. The proposed algorithms for image denoising provide satisfactory results. The good visual effect and PSNR of our proposed algorithm serve as important parameters to judge their performance.

Table 1. Comparison of the experimental results for "Boat" corrupted image with Gaussian noise with other standard methods

Gaussian- noise (σ)	PSNR (dB) (Jalab & Ibrahim, 2012)	PSNR (dB) (Cuesta et al., 2012)	PSNR (dB) Proposed FCE Filter
15	29.93	28.42	29.98
20	28.01	27.12	28.94
25	27.35	26.32	27.77

5. Discussion

An image denoising algorithms based on FCE is introduced. The structures of fractional masks are constructed by using n x n processing masks on four directions ($0,45^\circ,90^\circ,135^\circ$). The denoising performance is measured by conducting experiments according to visual perception and PSNR values. We analyze the influence of parameter $\wp$ for images corrupted by Gaussian noise with a σ value of 15 on the performance of PSNR denoising. The characteristic of the FCE filter can only be modified by changing the values of $\wp$ of the proposed masks. However, the main contribution of our paper was an image denoising algorithms based on FCE that is capable of denoising images corrupted by Gaussian noise. Our method could be applied as a pre-processing image enhancement procedure for image processing applications. Future works involve extending the proposed method for the texture enhancement, segmentation of digital images by using FCE method.

Conflict of Interests

The authors declare that there is no conflict of interests regarding the publication of this article.

Author Contributions

Both authors jointly worked on deriving the results and approved the final manuscript.

Acknowledgments

This research is supported by Project No.: RG312-14AFR from the University of Malaya.

References

Abreu, R., Stich, D., & Morales, J. (2013). On the generalization of the complex step method. *Journal of Computational and Applied Mathematics*, 241, 84–102.

Al-Mohy, A. H., & Higham, N. J. (2010). The complex step approximation to the Fréchet derivative of a matrix function. *Numerical Algorithms*, 53(1), 133–148.

Cuesta, E., Kirane, M., & Malik, S. A. (2012). Image structure preserving denoising using generalized fractional time integrals. *Signal Processing*, 92(2), 553–563.

Ibrahim, R. W. (2011). On generalized Srivastava-Owa fractional operators in the unit disk. *Advances in Difference Equations*, 2011(1), 1–10.

Ibrahim, R. W. (2012). Fractional complex transforms for fractional differential equations. *Advances in Difference Equations*, 2012(1), 1–12.

Ibrahim, R. W., & Jalab, H. A. (2013). The fractional complex step method. *Discrete Dynamics in Nature and Society, 2013*.

Jalab, H. A., & Ibrahim, R. W. (2012). Denoising algorithm based on generalized fractional integral operator with two parameters. *Discrete Dynamics in Nature and Society*, 2012.

Jalab, H. A., & Ibrahim, R. W. (2015a). Fractional Alexander polynomials for image denoising. *Signal Processing*, 107, 340–354.

Jalab, H. A., & Ibrahim, R. W. (2015b). Fractional Conway Polynomials for Image Denoising with Regularized Fractional Power Parameters. *Journal of Mathematical Imaging and Vision*, 51(3), 442–450.

Jumarie, G. (2006). Fractionalization of the complex-valued Brownian motion of order n using Riemann–Liouville derivative. Applications to mathematical finance and stochastic mechanics. *Chaos, Solitons & Fractals*, 28(5), 1285–1305.

Salagean, G. S. (1983). *Subclasses of univalent functions.* Paper presented at the Complex Analysis—Fifth Romanian-Finnish Seminar.